# PHASAR-based WDM-devices: principles, design and applications

# PHASAR-Based WDM-Devices: Principles, Design and Applications

Meint K. Smit, *Associate Member, IEEE,* and Cor van Dam

*(Invited Paper)*

***Abstract*—Wavelength multiplexers, demultiplexers and routers based on optical phased arrays play a key role in multiwavelength telecommunication links and networks. In this paper, a detailed description of phased-array operation and design is presented and an overview is given of the most important applications.**

## I. Introduction

COMMERCIAL interest in WDM components and systems is rapidly increasing. WDM provides a new dimension for solving capacity and flexibility problems in the telecommunication network. It offers a huge transmission capacity and allows for novel network architectures that offer much more flexibility than the current networks [16], [17]. Key components in WDM systems are the wavelength multiplexers and demultiplexers. Many principles have been proposed and reported for realization of multiplexers and demultiplexers. Commercially available components are based on fiber-optic or microoptic techniques [56], [57]. Research on integrated-optic (de)multiplexers has, since the early 1990's, increasingly been focused on grating-based and phased-array (PHASAR) based devices (also called arrayed waveguide gratings) [97]. Both are imaging devices, i.e., they image the field of an input waveguide onto an array of output waveguides in a dispersive way. In grating-based devices a vertically etched reflection grating provides the focusing and dispersive properties required for demultiplexing. In phased-array based devices these properties are provided by an array of waveguides, the length of which has been chosen such as to obtain the required imaging and dispersive properties. As phased-array based devices are realized in conventional waveguide technology and do not require the vertical etching step needed in grating-based devices they appear to be more robust and fabrication tolerant.

Phased array demultiplexers were proposed in 1988 by Smit [58]. The first devices operating at short wavelengths were reported by Vellekoop and Smit [93]–[95], [59]. Takahashi *et al.* reported the first devices operating in the long wavelength window [87], [88]. Dragone extended the phased-array concept from $1\times N$ to $N\times N$ devices, the so-called wavelength routers [27], [28] which play an important role in multiwavelength network applications.

Manuscript received July 23, 1996; revised November 7, 1996. Part of this work was carried out in the ACTS-BLISS AC-065 project.

The authors are with the Delft University of Technology, NL-2600 GA Delft, The Netherlands.

Publisher Item Identifier S 1077-260X(96)09506-8.

Devices reported so far can be divided into two main classes: silica-based devices and InP-based devices. Most of the silica-based devices employ fiber-matched (low-contrast) waveguide structures, which combine low propagation loss with a high fiber-coupling efficiency. More recently silicon-based polymer devices [32], [69] and lithiumniobate devices [53], [54] were reported which also employed fiber-matched waveguide structures.

Silica-based devices have relatively large dimensions due to the low index contrast and the corresponding large bending radii of the fiber-matched waveguides. This makes them less suitable for integration of large numbers of components on a single chip. Further, silica has a limited potential for integration of active functions due to its passive character. The feasibility of integration with switches, however, was demonstrated by Okamoto who reported successful integration of thermo-optical switches with phased-arrays in an integrated optical add-drop multiplexer [48], [49], [52].

The first InP-based PHASAR-demultiplexer was reported in 1992 by Zirngibl *et al.* [106]. InP-based devices have a better potential for integration of active functions. They exhibit higher propagation and fiber-coupling losses, however, the latter due to the small size of the waveguide cross section. Despite of the higher propagation losses the total on-chip device loss can be kept within acceptable limits due to the small component size which is possible because of the high-index contrast and which also allows for integrating larger numbers of components on a chip. InP-based demultiplexers cannot compete with silica-based devices with respect to fiber coupling loss, which makes them less suitable for realization of circuits with a low complexity. Their main advantage lies in their potential for monolithic integration of active components such as detectors [3], [4], [6], [74]–[76], [113], optical amplifiers and modulators [39]–[41], [108]–[112], [115], and switches [99], and their potential to integrate large numbers of components on a single chip.

Starting in 1993 [80], an increasing number of system experiments have been reported. The first silicon-based devices were recently introduced to the market. Integrated devices are still in a research stage but promise to provide the higher functionality which will be required in future telecommunication networks.

In this paper, we will review the present state-of-the-art for phased-array based devices. In Section II, the operation of the device will be described. Section III describes phased-array design for a number of different requirements, such as polarization independence, flattened wavelength response, low-loss, etc. Section IV describes a number of applications of phased-array demultiplexers. In Section V, a novel PHASAR-demultiplexer based on MMI-couplers is shortly described.

## II. Basic Operation

Fig. 1(a) shows the schematic layout of a PHASAR-demultiplexer. The operation is understood as follows. When the beam propagating through the transmitter waveguide enters the free propagation region (FPR) it is no longer laterally confined and becomes divergent. On arriving at the input aperture the beam is coupled into the waveguide array and propagates through the individual array waveguides to the output aperture. The length of the array waveguides is chosen such that the optical path length difference between adjacent waveguides equals an integer multiple of the central wavelength of the demultiplexer. For this wavelength the fields in the individual waveguides will arrive at the output aperture with equal phase (apart from an integer multiple of $2\pi$), and the field distribution at the input aperture will be reproduced at the output aperture. The divergent beam at the input aperture is thus transformed into a convergent one with equal amplitude and phase distribution, and an image of the input field at the object plane will be formed at the center of the image plane. The dispersion of the PHASAR is due to the linearly increasing length of the array waveguides, which will cause the phase change induced by a change in the wavelength to vary linearly along the output aperture. As a consequence, the outgoing beam will be tilted and the focal point will shift along the image plane. By placing receiver waveguides at proper positions along the image plane, spatial separation of the different wavelength channels is obtained.

In the following subsections, the most important properties of a PHASAR will be analyzed.

### A. Focusing

Focusing is obtained by choosing the length difference $\Delta L$ between adjacent array waveguides equal to an integer number of wavelengths, measured inside the array waveguides

$$\Delta L = m \cdot \frac{\lambda_c}{N_g} = \frac{mc}{N_g f_c} \tag{1}$$

in which $m$ is the order of the phased array, $\lambda_c(f_c)$ is the central wavelength (frequency) in vacuo, and $N_g$ is the effective index of the waveguide mode. With this choice the array acts as a lens with image and object planes at a distance $R_a$ of the array apertures.

The input and output apertures of the phased array are typical examples of Rowland-type mountings [43]. The focal line of such a mounting, which defines the image plane, follows a circle with radius $R_a/2$ as shown in Fig. 1(b). Transmitter and receiver waveguides should be positioned on this line.

### B. Dispersion and Free Spectral Range

From Fig. 1(b), it is seen that the dispersion angle $\theta$ resulting from a phase difference $\Delta\Phi$ between adjacent waveguides

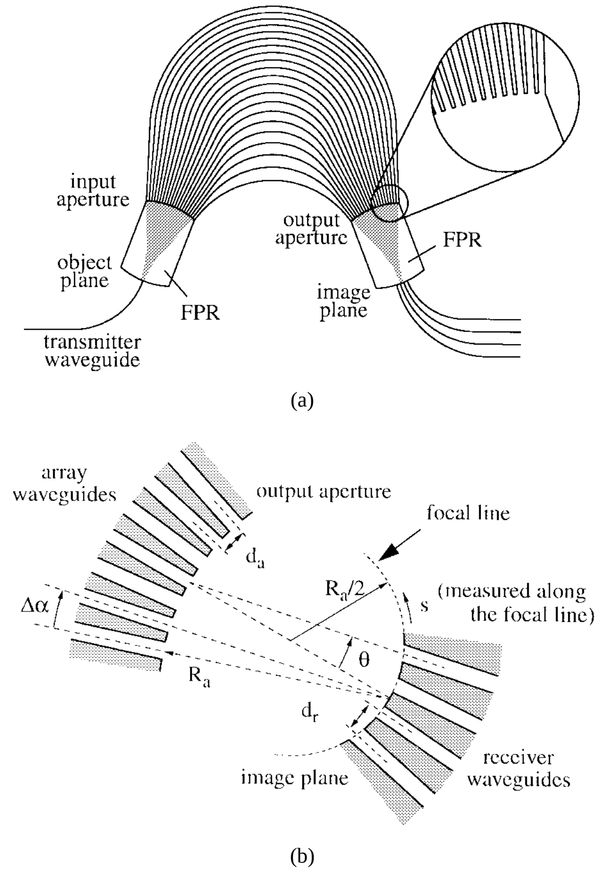


Fig. 1. (a) Layout of the PHASAR demultiplexer. (b) Geometry of the receiver side.

follows as

$$\theta = \operatorname{asin}\left(\frac{(\Delta\Phi - m2\pi)/\beta_{\mathrm{FPR}}}{d_a}\right) \approx \frac{\Delta\Phi - m2\pi}{\beta_{\mathrm{FPR}} d_a} \tag{2}$$

in which $\Delta\Phi = \beta\Delta L, \beta$ and $\beta_{\mathrm{FPR}}$ are the propagation constants of the waveguide mode and the slab mode in the free propagation region (FPR), respectively, and $d_a$ is the lateral spacing (on center lines) of the waveguides in the array aperture.

The dispersion $D$ of the array is described as the lateral displacement $ds$ of the focal spot along the image plane per unit frequency change. From Fig. 1(b), it follows (after some manipulation) that

$$D = \frac{ds}{df} = R_a \cdot \frac{d\theta}{df} = \frac{1}{f_c} \cdot \frac{\tilde{N}_g}{N_{\mathrm{FPR}}} \cdot \frac{\Delta L}{\Delta\alpha} \tag{3}$$

in which $f_c = c/\lambda_c$ is the central frequency, $N_{\mathrm{FPR}}$ is the (slab) mode index in the free propagation region, $\Delta L$ is the length increment of the array waveguides as described before, $\Delta\alpha = d_a/R_a$ is the divergence angle between the array waveguides in the fan-in and fan-out sections, and $\tilde{N}_g$ is the group index of the waveguide mode,

$$\tilde{N}_g = N_g + f\frac{dN_g}{df}. \tag{4}$$

It is seen that $R_a$ does not occur in the right-hand expression in (3) so that filling-in of the space between the array waveguides

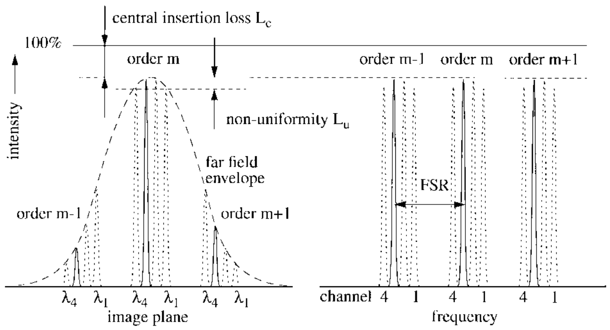


Fig. 2. Central insertion loss, nonuniformity and FSR. The 100% line denotes the peak intensity of the input field.

near the apertures due to a finite lithographical resolution does not affect the dispersive properties of the demultiplexer.

From (2), it is seen that the response of the phased array is periodical. After each change of $2\pi$ in $\Delta\Phi$ the field will be imaged at the same position. The period in the frequency domain, as shown in Fig. 2(b), is called the free spectral range (FSR). It is found as the frequency shift for which the phase shift $\Delta\Phi$ equals $2\pi$

$$\frac{2\pi\Delta f_{\rm FSR}}{c}\tilde{N}_g\Delta L = 2\pi \tag{5}$$

from which we find

$$\Delta f_{\rm FSR} = \frac{c}{\tilde{N}_g\Delta L} = \frac{f_c}{m'} \tag{6}$$

with $m' = (\tilde{N}_g/N_g)\cdot m$.

The rightmost identity, which is well known from grating theory, follows by substituting $\tilde{N}_g\Delta L = m'c/f_c$ [see (1)]. It is noted that for phased arrays, different from gratings, the FSR is not related to the order $m$ of the array, but to a modified order number $m'$, which can be interpreted as the order of the beam.

As the exact relation between $\theta$ and $\Delta\Phi$ is nonlinear [see (2)], (6) is only approximate and the FSR will be slightly dependent on the input and output ports. An accurate analysis is given by Takahashi *et al.* [91].

### C. Insertion Loss and Nonuniformity

Fig. 2(a) shows the field in the image plane for four different wavelengths. It is the sum-field of the far fields of all individual array waveguides. As the far-field intensity of the individual waveguides reduces away from the center of the image plane, as indicated in the figure, the focal sum-field will do the same. If the wavelength is changed it will move through the image plane and follow the envelope described by the far-field of the individual array waveguides. If we approximate the modal field of the array waveguides as a Gaussian beam, and neglect the effects of coupling on the beam shape, we can derive some simple analytical equations for estimating insertion loss, channel nonuniformity and bandwidth.

Using the Gaussian-beam approximation the intensity of the far-field is found from

$$I(\theta) = I_0 e^{-2\theta^2/\theta_0^2} \tag{7}$$

in which $\theta_0$ is the width of the equivalent Gaussian far field

$$\theta_0 = \frac{\lambda}{N_{\rm FPR}}\cdot\frac{1}{w_e\sqrt{2\pi}} \tag{8}$$

with $w_e$ the effective width of the modal field (as described in Appendix A). The nonuniformity $L_u$ is defined as the intensity ratio (in decibels) between the outer and the central channel. Using (7), the insertion loss of the receiver relative to the central channel is easily found by substituting the angle $\theta_{\max}$ $(\theta_{\max} \approx s_{\max}/R_a)$ corresponding to the outer receiver waveguide

$$L_u = -10\cdot\log\left(e^{-2\theta_{\max}^2/\theta_0^2}\right) \approx 8.7\cdot\theta_{\max}^2/\theta_0^2. \tag{9}$$

If the FSR is chosen equal to $N$ times the channel spacing $\Delta f$, as in wavelength routers (see Section IV-A), the excess loss $L_u$ of the outer channels will be close to 3 dB for reasons of power conservation: as for large numbers of channels receiver waveguide 1 and the virtual receiver $N+$ 1 will experience approximately the same loss, each of them has at least 3-dB excess loss relative to the central channel. For small values of $N$ the situation may be slightly better. Minimizing $L_u$ thus comes to increasing the FSR.

The insertion loss $L_0$ of the central channel is mainly determined by diffraction of light into undesired orders. The adjacent orders of the main focal spot will carry a fraction $\exp(-2\Delta\theta_{\rm FSR}^2/\theta_0^2)$, with

$$\Delta\theta_{\rm FSR} = \frac{\Delta s_{\rm FSR}}{R_a} = \frac{D}{R_a}\Delta f_{\rm FSR} \tag{10}$$

in which $D$ is the dispersion (3). If we neglect the power coupled into other orders the total loss $L_0$ can be estimated from

$$\begin{aligned} L_0 &\approx -10\cdot\log\left(1-4\cdot e^{-2\Delta\theta_{\rm FSR}^2/\theta_0^2}\right) + L_p \\ &\approx 17\cdot e^{-4\pi w_e^2/d_a^2} + L_p \end{aligned} \tag{11}$$

in which it has been assumed that $\exp(-2\Delta\theta_{\rm FSR}^2/\theta_0^2) \ll 1$. The factor 4 is due to the fact that power is lost in two orders, and equal losses occur (because of reciprocity) at both the input and the output side of the array. The term $L_p$ denotes the total propagation loss in the array and both FPR's due to absorption and scattering. From this equation it is seen that for low-loss devices the waveguide spacing $d_a$ in the array apertures should be minimal. For semiconductor-based devices best total loss reported is in the order of 2 dB [77]. It should be noted that (11) is a worst-case guess: coupling between the array waveguides will reduce the loss as discussed in Section III-E.

### D. Bandwidth

If the wavelength is changed the focal field of the PHASAR moves along the receiver waveguides. The frequency response of the different channels follows from the overlap of this field with the modal fields of the receiver waveguides. If we assume that the focal field is a good replica of the modal field at the input, and that the input and output waveguides are identical, the (logarithmic) transmission $T(\Delta f)$ around the channel maximum $T(f_c)$ follows as the overlap of the modal field with itself, displaced over a distance $\Delta s(\Delta f) = D\Delta f$

$$T(\Delta f) = T(f_c) + 20\log \int_{-\infty}^{+\infty} U(s)U(s - D\Delta f)ds \quad (12)$$

in which $U(s)$ is the normalized modal field, $D$ is the dispersion as defined in (3) and $T(f_c)$ is the transmission in dB at the channel maximum. For small values of $\Delta s$ (smaller than the effective mode width $w_e$) the overlap integral can be evaluated analytically by approximating the modal fields as Gaussian fields

$$T(\Delta f) - T(f_c) = 20\log\left(e^{-\frac{D\Delta f^2}{w_0^2}}\right) \approx -6.8 \cdot \left(\frac{D\Delta f}{w_e}\right)^2. \quad (13)$$

The $L$-dB bandwidth $\Delta f_L$ is twice the value $\Delta f$ for which $T(\Delta f) - T(f_c) = L$ dB

$$\Delta f_L = 0.77\frac{w_e}{D}\sqrt{L} = 0.77\frac{w_e}{d_r}\Delta f_{\rm ch}\sqrt{L}. \quad (14)$$

The latter identity follows by substitution of $D = d_r/\Delta f_{\rm ch}$. If we substitute $w_e/d_r \approx 0.4$ as a representative value (crosstalk due to receiver spacing $<-40$ dB, see Section II-E), the 1-dB bandwidth is found to be 0.31 $\cdot\Delta f_{\rm ch}$. For a channel spacing of 100 GHz we thus find a 1-dB bandwidth of 31 GHz.

### *E. Channel Crosstalk*

Crosstalk may be caused by many mechanisms. We will discuss six of them. The first four can be kept low by proper design. The other two follow from imperfections in the fabrication process and are more difficult to reduce.

It is usual in the literature on WDM devices to characterize the crosstalk performance by specifying the single channel crosstalk figure, i.e., the maximum crosstalk value which is measured with one active input channel. Under operating conditions the crosstalk will be higher than this value because all active input channels will contribute to it. An analysis of the crosstalk penalty under simultaneous multichannel operation is given by Takahashi *et al.* [91].

1) *Receiver Crosstalk:* The most obvious source of crosstalk is the coupling between the receivers through the exponential tails of the field distributions. This type of crosstalk directly follows from (12). Because we are now looking at the coupling through the exponential tails of the modal field the Gaussian approximation is not valid and the integral should be evaluated using the expressions for the (normalized) mode profile. In Fig. 3(a) the crosstalk due to overlapping fields has been calculated for different lateral $V$-parameters. The curves are almost polarization independent. Note that in polarization dependent waveguides the lateral $V$-parameter will be polarization dependent.
2) *Truncation:* Another source of crosstalk results from truncation of the field due to the finite width of the array aperture. This causes power to be lost at the input aperture, and at the output aperture the sidelobe level of the focal field will increase. For a proper PHASAR design, the array aperture angle should be chosen such that the corresponding crosstalk is sufficiently low. Fig. 3(b) shows the transmitted power (solid line) and the crosstalk versus the array aperture half angle $\theta_a$, normalized to the Gaussian width $\theta_0$ as defined in (8), for different values of the relative receiver spacing $d_r/w$. The values shown are calculated for input and output waveguides with $V = 3$. As the estimation of Fig. 3(a) is rather pessimistic, it is best to use the envelope depicted by the bold line. The dependence on the $V$-parameter is small. The envelope of the crosstalk curves (bold line) can be used for extimating the maximum crosstalk level. It is seen that for $\theta_a > 2\theta_0$ the truncation crosstalk is less than $-35$ dB.
3) *Mode Conversion:* If the array waveguides are not strictly single mode a first-order mode excited at the junctions between straight and curved waveguides can propagate coherently through the array and cause “ghost” images. Because of the difference in propagation constant between the fundamental and the first-order mode these images will occur at different locations and the “ghost image” may couple to an undesired receiver thus degrading the crosstalk performance. Mode conversion can be kept small by optimising the offset at the junctions on minimal first-order mode excitation.
4) *Coupling in the Array:* Crosstalk can also be incurred by phase distortion due to coupling in the input and output sections in the arrays. It might be expected that this type of coupling will not heavily affect the focusing and dispersive properties of the array on similar grounds as mentioned under (3) and (4). The filling in of the gaps near the array apertures can be considered as introducing an extremely strong coupling in the input and output region, which obviously does not degrade the PHASAR performance [59]. Day *et al.* [24] observe a degradation of the crosstalk performance using BPM-simulation, however.
5) *Phase Transfer Incoherence:* A fifth source of crosstalk results from incoherence of the phased array due to imperfections in the fabrication process. The optical path length of the array guides is in the order of several thousands of wavelengths. Deviations in the propagation constant may lead to considerable errors in the phase transfer, and, consequently, to an increase of the crosstalk level. Takada *et al.* [86] and Yamada *et al.* [101], [102] have shown that improved crosstalk is feasible by correcting the phase errors. Phase errors may be caused by small deviations in the effective index, due to local variations in composition, film thickness or waveguide width, or by inhomogeneous filling in of the gap near the apertures of the phased array. Also more systematic errors, e.g., due to discretization in the mask pattern generation may contribute to the crosstalk [24].
6) *Background Radiation:* As a last possible source of crosstalk, we mention background radiation due to

light scattered out of the waveguides at junctions or rough waveguide edges. This is especially important in waveguide structures where the light is also guided besides the waveguides, e.g., in shallowly etched ridge guides or in waveguides structures on a heavily doped substrate where the undoped buffer layer may also act as a waveguide.

Crosstalk in practical devices is not limited by design but by imperfections in the fabrication process. Typical crosstalk values reported for PHASAR-demultiplexers are in the order of −25 dB for InP-based devices to better than −30 dB for silica-based devices. Recent experiments in our laboratory show crosstalk levels better than −30 dB also for good semiconductor devices. Improvement of these figures is mainly a matter of improving fabrication technology.

### *F. Polarization Dependence*

Phased arrays are polarization independent if the array waveguides are polarization independent, i.e., the propagation constants for the fundamental TE- and TM-mode are equal. Waveguide birefringence, i.e., a difference in propagation constants, will result in a shift $\Delta f_{\mathrm{pol}}$ of the spectral responses with respect to each other, which is called the polarization dispersion. It can be calculated if we consider the wavelengths in the waveguide. Light with different wavelengths *in vacuo* will be coupled into the same receiver waveguide, if the wavelengths $\lambda_{\mathrm{TE}}$ and $\lambda_{\mathrm{TM}}$ of the fundamental modes in the waveguide are equal

$$\begin{aligned}\lambda_{\mathrm{TM}}(f) &= \frac{c}{f\cdot N_{\mathrm{TM}}(f)} = \lambda_{\mathrm{TE}}(f-\Delta f_{\mathrm{pol}})\\ &= \frac{c}{(f-\Delta f_{\mathrm{pol}})\cdot N_{\mathrm{TE}}(f-\Delta f_{\mathrm{pol}})}\end{aligned} \tag{15}$$

in which $N_{\mathrm{TE}}$ and $N_{\mathrm{TM}}$ are the effective indices for both polarizations. By solving $\Delta f_{\mathrm{pol}}$ from (15), we find

$$\Delta f_{\mathrm{pol}} \approx f\cdot\frac{(N_{\mathrm{TE}}-N_{\mathrm{TM}})}{\tilde{N}_{\mathrm{TE}}} \tag{16}$$

in which $\tilde{N}_{\mathrm{TE}}$ is the group index. For InGaAsP–InP DH waveguide structures $\Delta f_{\mathrm{pol}}$ is typically in the order of 4–5 nm. For silica-based and, more generally, for low-contrast waveguides, it will be much smaller. Also in waveguides structures which are designed for polarization independence polarization dependence may occur due to strain induced during the fabrication process. A number of methods to reduce polarization dependence will be discussed in Section IV.

## III. Phased-Array Design

### *A. Specification*

A PHASAR is specified by the following characteristics:

- number of channels $N$;
- central frequency $f_c$ and channel spacing $\Delta f_{\mathrm{ch}}$;
- $L$-dB channel bandwidth $\Delta f_L$;
- free spectral range $\Delta f_{\mathrm{FSR}}$;
- maximal insertion loss $L_0$ of the central channel;
- maximal nonuniformity $L_u$;

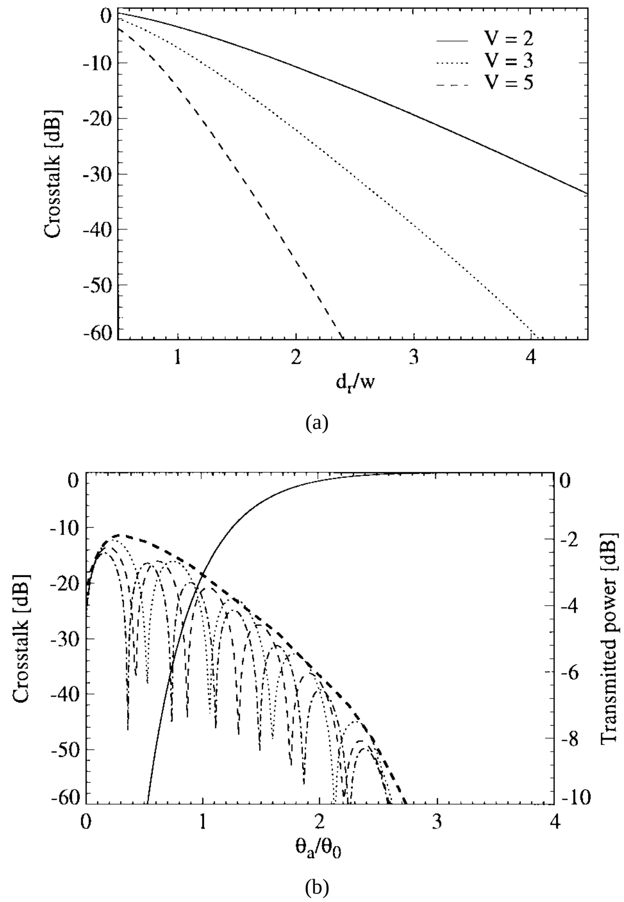


Fig. 3. (a) Crosstalk resulting from the coupling between two adjacent receiver channels for different values of the lateral $V$-parameter of the receiver waveguides. (b) Transmitted power (solid line) and crosstalk as a function of the relative array aperture $\theta_a/\theta_0$, for different values of the relative receiver spacing $d_r/w$ ($d_r/w$ = 2.5, 3.0, 3.5). The values shown are calculated for input and output waveguides with $V$ = 3. The bold line indicates the envelope of the crosstalk curves (maximum crosstalk level).

- maximal crosstalk level;
- maximal polarization dependence.

It is noted that the nonuniformity and the FSR can not be chosen independent from each other (see Section IV-A).

### *B. Demultiplexer Design Procedure*

PHASAR's have many degrees of design freedom, and many design approaches are possible. The approach followed at Delft University of Technology for designing multiplexers and demultiplexers is explained below. It starts from a given waveguide structure (i.e., waveguide width $w$ and lateral $V$-parameter fixed). The design parameters of the PHASAR are derived subsequently from the design specifications. For design of a wavelength router the procedure is slightly different (see Section IV-A).

- *Receiver Spacing $d_r$:* We start with the crosstalk specification, which puts a lower limit on the receiver spacing $d_r$. As with todays technology crosstalk levels lower than −30 to −35 dB are difficult to realize it does not make sense to design the array for much lower crosstalk. To be on the safe side we take a margin of 5–10 dB and

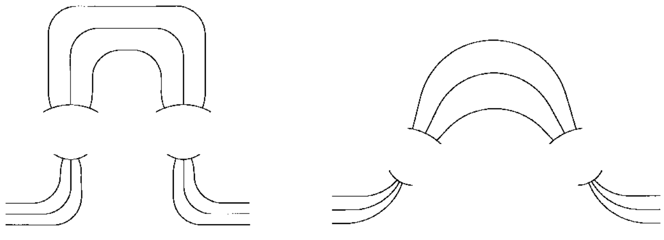


Fig. 4. Phased-array waveguide geometries.

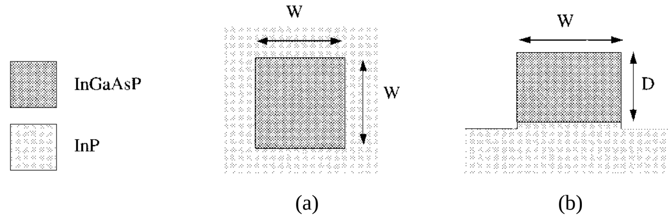


Fig. 5. Zero-birefringent waveguide structures: (a) Buried waveguide, and (b) raised-strip waveguide.

read from Fig. 3(a) the ratio $d_r/w$ required for $-40$ dB crosstalk level. It is noted that the crosstalk for TE- and TM-polarization may be different because the lateral index contrast and, consequently, the lateral $V$-parameter can differ substantially for the two polarizations.

- *FPR Length $R_a$:* From the maximum acceptable excess loss for the outer channel (the nonuniformity $L_u$) we determine the maximum acceptable dispersion angle $\theta_{\max}$ using (8) and (9). The minimal length $R_a$ of the free propagation region (FPR) then follows as $R_a = s_{\max}/\theta_{\max}$ in which $s_{\max}$ is the $s$-coordinate of the outer receiver (see Fig. 1(b)).
- *Length Increment $\Delta L$:* First we compute the required dispersion of the array from $D = ds/df = d_r/\Delta f_{\mathrm{ch}}$ [see (3)]. The waveguide spacing $d_a$ in the array aperture should be chosen as small as possible (a large spacing will lead to high coupling losses from the FPR to the array and vice versa). With $d_a$ and $R_a$ fixed the divergence angle $\Delta\alpha$ between the array waveguides is fixed: $\Delta\alpha = d_a/R_a$ [see Fig. 1(b)] and the length increment $\Delta L$ of the array follows from (3).
- *Aperture Width $\theta_a$:* The angular half width $\theta_a$ of the array aperture should be determined using a graph as Fig. 3(b) (adapted for the specific waveguide structure used).
- *Number of Array Waveguides $N_a$:* The choice of $\theta_a$ fixes the number of array waveguides: $N_a = 2\theta_a R_a/d_a + 1$.

This completes the determination of the most important geometrical parameters of the PHASAR. For the array waveguides a number of different shapes can be applied to realize the length increment $\Delta L$. Takahashi *et al.* [88] used the geometry as depicted in Fig. 4(a) which is very simple from a design point of view, with a constant $R$ for all array arms. Smit [59] and Dragone [27] applied the geometry of Fig. 4(b), which contains a minimum number of waveguide junctions. This is especially important in semiconductor waveguides where junction losses and mode conversion at junctions can degrade the PHASAR performance.

The freedom in the choice of the array shape is bounded by the requirement that the array waveguides should not come too close to each other. For low-dispersion values, e.g., for duplexing 1.3 and 1.55 $\mu$m, the shapes as depicted in Fig. 4 are not suitable; the array waveguides come too close together or will even intersect. Adar *et al.* [1] applied S-bend like arrays in which the dispersion of one curved section is reduced by a second section with opposite curvature and, consequently, opposite $\Delta L$. More complex shapes have been reported, too [44], [45].

### C. Design for Polarization Independence

Several methods can be applied for eliminating the polarization dependence of the response due to waveguide birefringence. Five different methods will be discussed

1) *Nonbirefringent Waveguides:* The most obvious way to make a PHASAR polarization independent is by eliminating the birefringence of the waveguide. This can be done by making the waveguide cross section square if the index contrast is the same in the vertical and lateral direction as, for example, in buried waveguide structures. Small deviations of the square shape, for example due to nonperfect control of the waveguide width, will disturb the polarization independence. If the index contrast between core and cladding is high the tolerance requirements on waveguide width control become impractically tight. Tolerant design requires, therefore, low-contrast waveguides with a relatively large waveguide core (which is advantageous for achieving low-fiber coupling loss). Bellcore [8], [63] recently reported a polarization independent device based on a buried InGaAsP–InP waveguide structure with a low-contrast waveguide core (small GaAs-fraction), as shown in Fig. 5(a). Philips and TU Delft [6], [13]–[15], [62], [96] reported several devices based on a raised strip guide [shown in Fig. 5(b)] using similar material for the waveguide core. The birefringence induced by the asymmetry in lateral and vertical index contrast, which occurs in this waveguide, was compensated by a small correction of the aspect ratio (height/width) of the waveguide core. An advantage of the raised strip guide is that, due to the high lateral index contrast, it allows for very short bending radii and, consequently, compact design.

Attempts have been made to compensate the birefringence of conventional "flat" waveguide structures by applying strained MQW-waveguides. Compressive strain, obtained by increasing the Ga-fraction, increases the birefringence, whereas tensile strain reduces it. First results of this method show that polarization dispersion changes in the order of 7–12 nm are possible [98]. A complication of this approach is that the intrinsic birefringence of MQW-structures is considerably higher than that of quaternary bulk material and requires very high strains to be compensated. This makes the approach very sensitive to well-width and composition control.

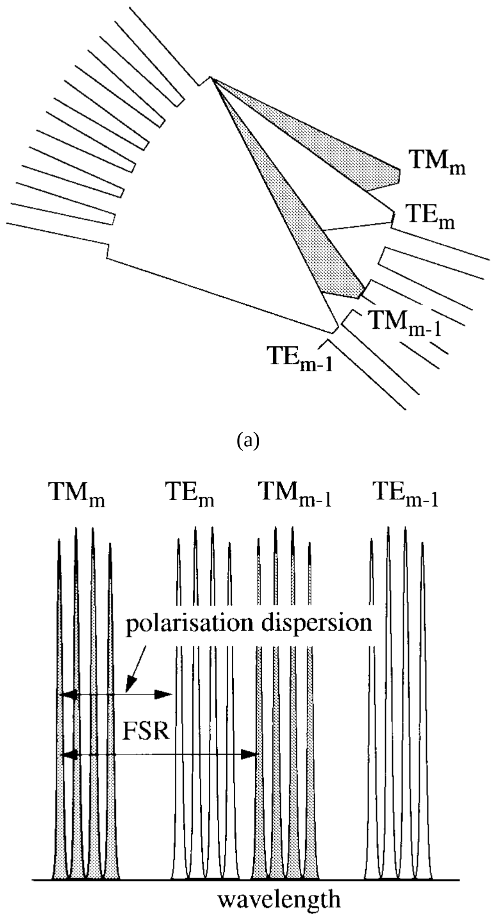


Fig. 6. Schematic diagram of the different diffraction orders at the receiver side for both states of polarization: Polarization dispersion.

The birefringence problem occurs also in silica-based waveguides, where it is due to strain induced by the different thermal expansion coefficients of silica and silicon. It can be reduced by using silica substrates instead of silicon substrates [78].

2) *Order Matching:* The first attempt to make PHASAR's polarization independent was based on matching the FSR to the polarization dispersion as shown in Fig. 6 [66], [71], [94], [95], [107].

If the FSR is chosen equal to the polarization dispersion the $m$th-order beam for TE will overlap with the TM-polarized beam of order $m-$ 1, which makes the response virtually polarization independent. From (6), it is seen that this is obtained by choosing

$$\Delta L = \frac{c}{\tilde{N}\Delta f_{\mathrm{pol}}}. \tag{17}$$

For this design the procedure described in Section III-B should be slightly changed. By fixing the incremental length according to (17) the divergence angle $\Delta\alpha$ is fixed through (3) and $R_a$ through $R_a = d_a/\Delta\alpha$ [see Fig. 1(b)]. $R_a$ being fixed in this way the nonuniformity $L_u$ can no longer be freely chosen. A disadvantage of this method is that the total wavelength span available

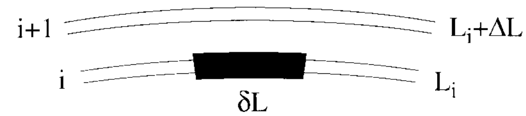


Fig. 7. Schematic diagram of the birefringence compensation principle.

for the WDM channels is limited by the polarization dispersion which is in the order of 4–5 nm for conventional InGaAsP–InP DH structures. Another disadvantage is that the exact value of the polarization dispersion is very sensitive to variations in layer composition and thickness, which makes it difficult to obtain a good match.

3) *Halfwave Plate:* A very elegant method is the insertion of a $\lambda/2$-plate in the middle of the phased array. Light entering the array in TE-polarized state will be converted by the $\lambda/2$-plate and travel through the second half of the array in TM-polarized state, and TM-polarized light will similarly traverse half the array in TE-state. As a consequence TE- and TM-polarized input signals will experience the same phase transfer regardless of the birefringence properties of the waveguides applied. This method was proposed by Takahashi *et al.* [89] and using polyimide halfwave plates it has been successfully applied to silica-based [33], [50] and $LiNbO_3$-based devices [53], [54].

As the polyimide halfwave plates have a thickness of more than 10 $\mu$m, they are only applicable to waveguide structures with a small NA that can bridge this distance with small diffraction losses. In semiconductor waveguides, the method is not practical due to the large NA of these waveguides. It could be applied successfully there too if a compact and fabrication tolerant integrated polarization converter can be developed.

4) *Dispersion Compensation:* In semiconductor-based PHASAR's a broad-band solution for the polarization dependence problem is found in compensation of the polarization dispersion by inserting a waveguide section with a different birefringence in the phased array. The method was proposed for silica-based waveguides by Takahashi *et al.* [90] and successfully applied to InP-based devices by Zirngibl *et al.* [114].

The operation can be explained by considering the phase transfer difference $\Delta\Phi$ between two adjacent waveguides, in one of which a section with length $\delta L$ with a different birefringence is inserted (see Fig. 7)

$$\Delta\Phi = k_0[N_g\Delta L + \delta L(N_g - n_g)] \tag{18}$$

in which $N_g$ and $n_g$ are the effective mode indices of the original waveguide and the compensation section. It is easily verified that $\Delta\Phi$ becomes polarization independent if $\delta L$ is chosen according to

$$\delta L = \Delta L \bigg/ \left(\frac{\Delta n}{\Delta N} - 1\right) \tag{19}$$

in which $\Delta N$ and $\Delta n$ are the differences between the TE and the TM-value of $N_g$ and $n_g$, respectively. The whole

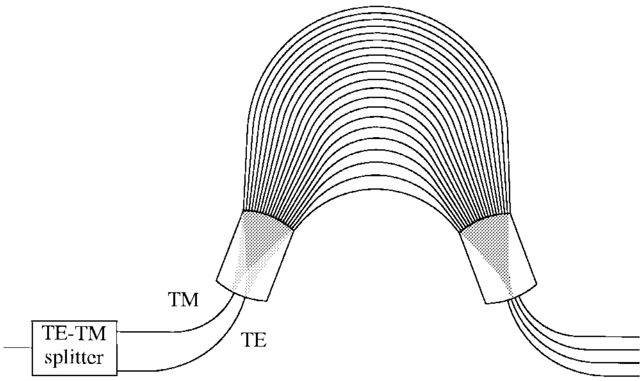


Fig. 8. Application of a polarization splitter at the input.

array can be made polarization independent by inserting a section with length $\delta L$ in the first waveguide, $2\delta L$ in the second one, $3\delta L$ in the third one, and so on. The compensation section will thus obtain a triangular shape and its total length will amount to $N_a\delta L$, in which $N_a$ is the number of array waveguides. The method applies for both positive and negative values of $\Delta n/\Delta N$. For values close to 1, the compensation section will become excessively long. A disadvantage is that $\Delta N$ and $\Delta n$ are very sensitive to film thickness and waveguide width, so that the compensation requires tight control of these parameters.

5) *Polarization Splitter:* Another method for obtaining polarization independence is by applying a polarization splitter at the input, as shown in Fig. 8. Due to the polarization dispersion the position of the focal spot in the image plane for TE polarization is shifted relative to the TM-polarized one. If the distance between the TE and the TM-polarized receiver in the object plane is chosen equal to the polarization dispersion in the image plane, the TE and TM-polarized signals will focus on the same position and the response will become polarization independent over a broad wavelength range. The method does not apply to $N \times N$ devices.

### D. Design for Flattened Response

In many applications, a flattened passband is important in order to relax the requirements on wavelength control. Three methods to achieve this goal will be discussed.

1) *Multimode Receiver Guideş.* The most simple method is the use of broad (multimode) waveguides at the receiver side [5], [66], [67], [74], [75]. If the focal spot moves along these broad receivers almost 100% of the light will be coupled into the receiver over a considerable part of the receiver aperture, thus causing a flat region in the frequency response as shown in Fig. 9(a). In this way, the 1-dB bandwidth can easily be increased from 31% of the channel spacing, as shown in Section II-D for a nonflattened PHASAR, to more than 65%.

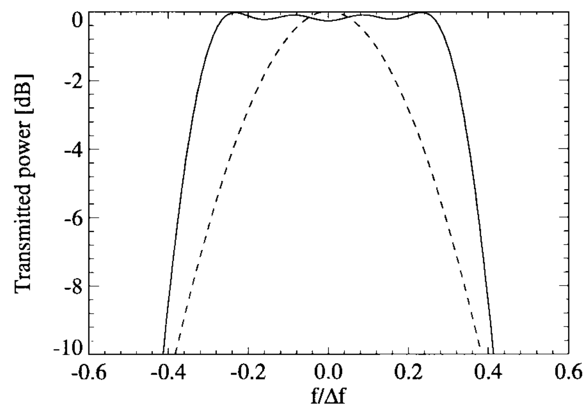


(a)

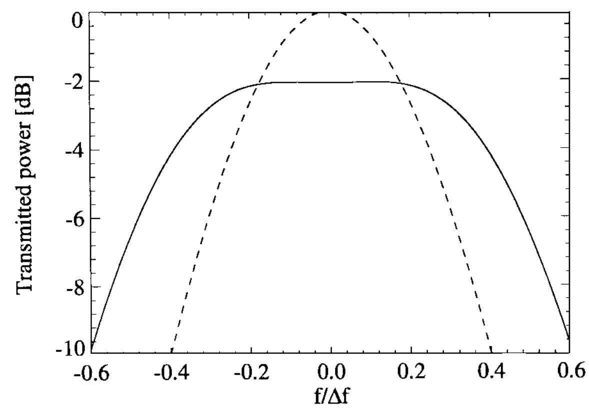


(b)

Fig. 9. Flattening of the wavelength response by (a) using multimode receiver waveguides, and (b) applying an MMI-powersplitter at the transmitter side. The dashed lines indicate the response without flattening.

Due to the multimode character of the receiver waveguides this method can only be applied at the receiver side of a WDM-link, where the multimode waveguides can be coupled to a detector without additional signal loss.

2) *MMI-Flattening:* A flattened response with single-mode outputs can be obtained by applying a short multimode interference (MMI) power splitter at the end of the transmitter waveguide [7], [64], [65]. This device converts the single waveguide mode at the input of the cou-pler into a double image. The resulting output field pattern has a "camel-like" shape and the depth of the central depression can be controlled with the MMI width. If the image of this "camel-shaped" field moves along the single mode receivers the response will have a flat region as shown in Fig. 9(b). This method of flattening introduces insertion loss due to the mismatch between the "camel-shaped" focal field and the receiver mode.

A similar effect can be obtained by applying a $Y$-junction and bringing the two output branches close together in the transmitter aperture. This method is less compact and less robust, however.

3) *Shaping the Phase Transfer:* As the field in the image plane is the Fourier transform of the field at the output

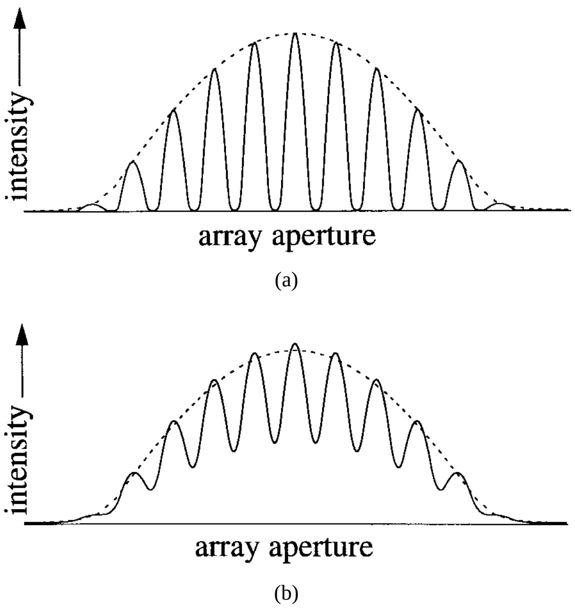


Fig. 10. Fields at the input (dashed) and the output aperture (solid) of the phased array for (a) a waveguide structure with strong confinement, and (b) a structure with moderate confinement. For efficient coupling to the receiver waveguides the output field should follow the dashed lines.

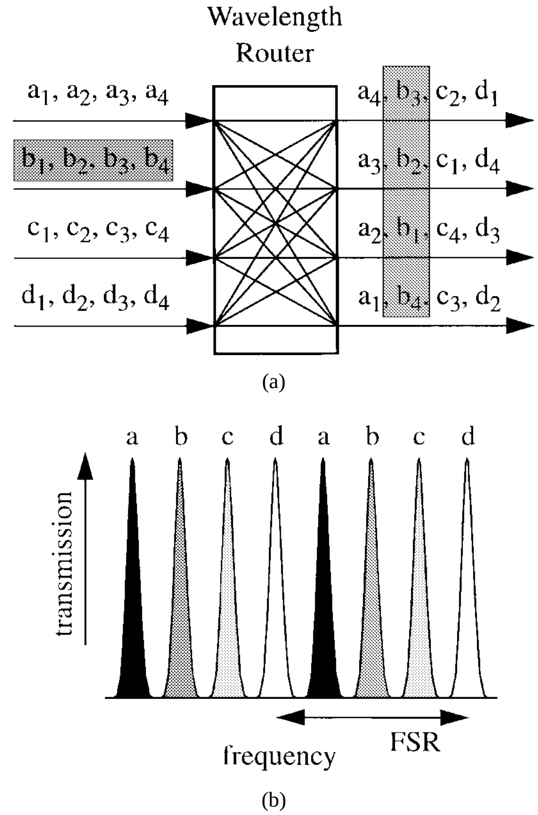


Fig. 11. Schematic diagram illustrating the operation of a wavelength router: (a) Interconnectivity scheme ($a_i$ denotes the signal at input port $a$ with frequency $i$) and (b) frequency response.

aperture, a more or less rectangular field can be realized if the field at the output aperture has a $\sin(x)/x$ distribution ($x$ measured along the aperture). Such a sinc distribution can be approximated in a discrete manner by multiplying the field at the array aperture with a function with alternating sign, in such a way that the Gaussian-like field is converted into a $\sin(x)/x$-like field with positive and negative sidelobes. The multiplication can be realized by inserting an additional half wavelength in the array waveguides terminating in the negative sidelobe regions or by increasing the optical length using thermo-optic or photo-elastic effects [46].

### *E. Design for Low Loss*

For properly designed PHASAR's realized with low-loss waveguides the total loss is dominated by the loss occurring at the junctions between the array and the FPR. Low losses can be obtained if the transition from the array to the FPR is adiabatical, i.e., if the gap between the waveguides reduces linearly to zero. Due to the finite resolution of the lithographical process the gap between the waveguides will stop abruptly, however, when the waveguides come too close together. At this discontinuity the field coming out of the array will show a modulation that is dependent on the width of the gap between the array waveguides and on the confinement of the field in the guides. Fig. 10 shows the field for a large and a smaller gap. Due to the ripple in the field pattern a considerable fraction of the power will diffract into adjacent orders and be lost. On reciprocity grounds an equal loss will occur at the input aperture.

To reduce this loss, the ripple of the output field should be reduced. This can be obtained by reducing the gap width (which requires better lithography) or by reducing the confinement of the waveguides. A disadvantage of the latter approach is that lowering the confinement increases the minimal bending radius and, consequently, increases the device size. Low confinement can be combined with small bending radii by applying a local contrast reduction near the array apertures using a double-etch process [23].

## IV. Applications

In addition to the basic functions of wavelength multiplexing and demultiplexing, PHASAR's are applied in wavelength routers and, in combination with other components such as amplifiers and switches, in more complex devices for use in multiwavelength networks. In this section a number of applications will be discussed.

### *A. Wavelength Routers*

Wavelength routers were first reported by Dragone [27], [28]. They provide an important additional functionality as compared to multiplexers and demultiplexers and play a key role in more complex devices as add-drop multiplexers and wavelength switches. Fig. 11 illustrates their functionality. Wavelength routers have $N$ input and $N$ output ports. Each of the $N$ input ports can carry $N$ different frequencies. The $N$ frequencies carried by input channel 1 are distributed among output channels 1 to $N$, in such a way that output channel 1 carries frequency $N$ and channel $N$ frequency 1. The $N$ frequencies carried by input 2 are distributed in the same way, but cyclically rotated by 1 channel in such a way that frequencies 1–3 are coupled to ports 3–1 and frequency 4 to port 4. In this way each output channel receives $N$ different frequencies, one from each input channel. To realize such an interconnectivity scheme in a strictly nonblocking way using a single frequency a huge number of switches would be required. Using a wavelength router, this functionality can be achieved using only one single component.

A wavelength router is obtained by designing the input and the output side of a PHASAR symmetrically, i.e., with $N$ input and $N$ output ports. For the cyclical rotation of the input frequencies along the output ports, as described above, it is essential that the frequency response is periodical as shown in Fig. 11(b), which implies that the FSR should equal $N$ times the channel spacing. From (6), it is seen that this is obtained by choosing

$$\Delta L = \frac{c}{\tilde{N}_g N \Delta f_{\mathrm{ch}}} \tag{20}$$

in which $\tilde{N}_g$ is the group index of the waveguide mode, $N$ is the number of frequency channels and $\Delta f_{\mathrm{ch}}$ is the channel spacing. For this design the procedure described in Section III-B should be changed in a similar way as described in Section III-C-2. By fixing the incremental length according to (20) the divergence angle $\Delta\alpha$ is fixed through (3) and $R_a$ through $R_a = d_a/\Delta\alpha$ [see Fig. 1(b)]. With this choice of the FSR the nonuniformity $L_u$ is fixed and will be in the order of 3 dB, which can be seen as follows. Channels at a frequency $\Delta f_{\mathrm{FSR}}/2$ away from the central frequency will experience an excess loss $L_u$ of at least 3 dB because the focal spot corresponding to this frequency will be equally divided among two orders which focus symmetrically around the center of the image plane. As in a periodical design the frequency spacing between the outer channels comes close to the FSR, the outer channels will experience an excess loss $L_u$ in the order of 3 dB.

Wavelength routers have been applied in various configurations in add-drop multiplexers and wavelength selective switches [29], [30], [37], [38], [49], [68], [79]–[83] and in multiwavelength networks [31]. In combination with a DFB laser used as a wavelength converter a wavelength router has also been applied as a wavelength switch [68], [72].

### B. Multiwavelength Receivers

A multiwavelength receiver is obtained by integration of a demultiplexer with a photodiode array. The first PHASAR receiver, reported in 1993 by Amersfoort *et al.* [3], [4], applied a twinguide waveguide structure in which the passive region was obtained by locally removing the absorbing top layer. Integrated receivers have also been realized in buried waveguide structures [113] and in polarization independent raised-strip waveguides [6], [62]. A wavelength-flattened receiver module hybridly integrated with a silicon bipolar frontend array has been reported by Steenbergen *et al.* [74], [75], [76]. Recently, a low-loss (3 dB on-chip loss) ei-channel WDM receiver with 10 GHz bandwidth per channel has been reported [77].

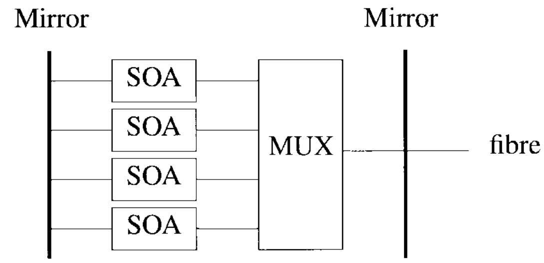


Fig. 12. Integrated multiwavelength laser.

### C. Multiwavelength Lasers

Todays WDM systems use wavelength-selected or tunable lasers as sources. Multiplexing of a number of wavelengths into one fiber is done using a power combiner or a wavelength multiplexer. Integrated multiwavelength lasers have been realized by combining a DFB-laser array (with a linear frequency spacing) with a power combiner on a single chip [9], [103], [104].

Using a power combiner for multiplexing the different wavelengths in a single fiber is a very tolerant method but it introduces a loss of 10 $\cdot \log N$ dB, $N$ being the number of wavelength channels. The combination loss can be reduced by applying a wavelength multiplexer at the cost of more stringent requirements on the control of the laser wavelengths, however.

An elegant solution to this problem is combining a broad-band optical amplifier array with a multiplexer into a Fabry–Perot cavity as depicted in Fig. 12. This principle was first demonstrated in the MAGIC-laser [100] in a hybridly integrated form. If one of the semiconductor optical amplifiers (SOA's) is excited the device will start lasing at the passband maximum of the multiplexer channel to which the SOA is connected. All SOA's can be operated and (intensity) modulated simultaneously, in principle. An important advantage of this component is that the wavelength channels are automatically tuned to the passbands of the multiplexer and coupled to the single output port with low loss.

Zirngibl and Joyner reported the first multiwavelength lasers based on integration of a SOA-array with a PHASAR [39], [108], [110] and demonstrated it in a 9 $\times$ 200 Mb/s transmission experiment [113]. Despite of their long cavity length these lasers show single mode operation in a wide range of operating conditions [112]. Direct modulations speeds in excess of 1 Gb/s were recently reported [115]. Power coupled into a fiber is still low. Highest power reported so far is 0.15 mW [70], [73].

Joyner *et al.* [41] reported integration of a MW-laser with an electroabsorption modulator. They used the power radiated into an adjacent order of the phased array to couple light out of the cavity into the modulator.

A problem in MW-lasers with a small FSR is that the laser may start lasing in a wrong order and, consequently, at a wrong frequency. Doerr *et al.* [26] proposed and demonstrated a method to suppress the transmission for undesired orders by chirping the incremental length $\Delta L$ in the array.

Tachikawa *et al.* [83] reported a 32-channel discretely tunable laser based on a 4 $\times$ 8 PHASAR with 12 SOA's with

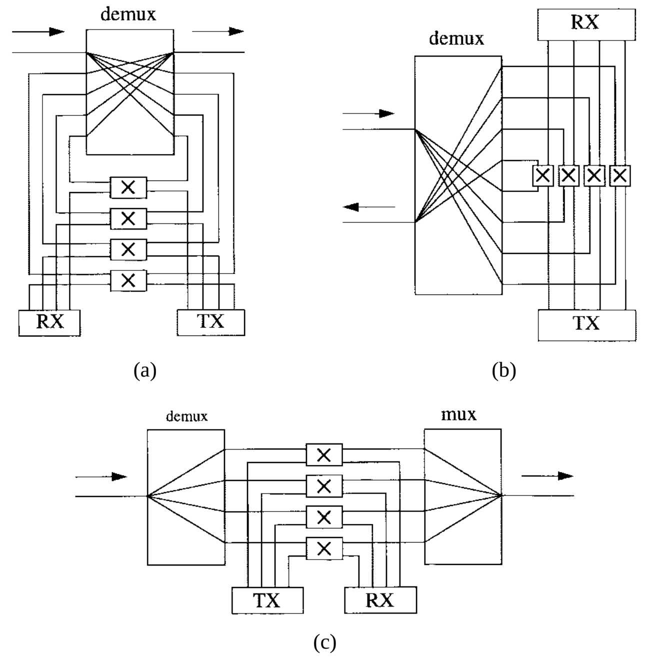


Fig. 13. Three different ADM configurations: (a) Loop-back, (b) fold-back, and (c) cascaded demux/mux.

one reflecting mirror connected to both the 4-input and the 8-output ports. The 32 wavelengths are generated by powering the proper SOA pairs.

### D. Wavelength-Selective Switches and Add–Drop Multiplexers

Add-drop multiplexers (ADM's) form a special class of wavelength selective switches. They are used for coupling one or more wavelength signals from a main input port to one or more drop ports by operating the corresponding switches. Simultaneously, the other signals are routed to the main output port, together with the signals applied at the proper add ports. In Fig. 13(a) the configuration as realized by Tachikawa *et al.* [80], [82], [85] is shown. The realized device (hybridly integrated, in which the switching was done by changing fiber connectors), showed a fiber-to-fiber insertion loss of 3–4 dB for the add/drop signals and 6–8 dB for the transmitted signals. By a suitable arrangement of the loop-back optical paths the insertion loss difference between the transmitted signals can be minimized [35].

A disadvantage of this loop-back configuration is that the crosstalk of the PHASAR is coupled directly into the main output port. This problem can be reduced by applying the PHASAR in a fold-back configuration as shown in Fig. 13(b) [29], [37]. A third approach is using a separate demultiplexer and multiplexer [Fig. 13(c)] as reported by Okamoto *et al.* [48], [49], [52]. The two PHASAR's employed in this approach were placed close together in order to ensure that their channel frequencies match.

In wavelength routed networks, spatial switching of arbitrary wavelength signals between multiple channels allows for efficient use of the transmission capacity using a fixed number of wavelengths and re-using them. For this approach, a number of configurations using silica-based waveguide structures have been reported [36], [37], [79].

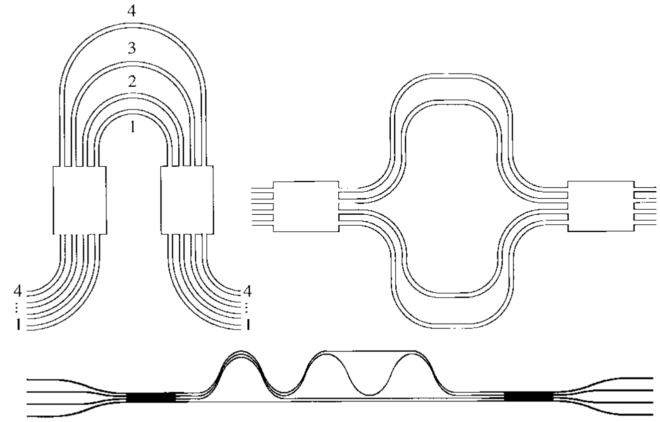


Fig. 14. MMI-based PHASAR configuration.

TABLE I
PHASE DIFFERENCES $\Delta\varphi_{ij}$ BETWEEN INPUT PORT $i$ AND $j$, REQUIRED FOR POWER RECOMBINATION IN THE DIFFERENT OUTPUT PORTS OF A $4 \times 4$ MMI COUPLER

| | | | | | | | | | | |
|---|---|---|---|---|---|---|---|---|---|---|
| $\Delta\varphi_{12}$ | 45 | -90 | -45 | -90 | -135 | -90 | 135 | -90 | 45 |
| $\Delta\varphi_{23}$ | 180 | -180 | 0 | -180 | 180 | -180 | 0 | -180 | 180 |
| $\Delta\varphi_{34}$ | 135 | -270 | -135 | -270 | -45 | -270 | 45 | -270 | 135 |
| output port | 1 | | 2 | | 4 | | 3 | | 1 |

## V. MMI-BASED PHASAR's

Recently, a novel type of PHASAR-based on MMI-couplers was proposed and experimentally demonstrated on InP [22], and a design for a low-contrast waveguide structure has been proposed [42]. It is obtained by replacing the FPR's of the "classical" PHASAR by MMI-couplers. Fig. 14 shows three different realizations. The operation can be understood as follows. Conventional MMI-couplers divide the power applied to an input port equally among all $N$ output ports [61], but with a different phase for each port [10]. To each input port corresponds a specific set of phases at the output port. If $N$ signals with this specific phase set (with a minus sign) are applied to the input port all power will recombine in the corresponding output port, due to reciprocity. This is shown in Table I. If we apply, for example, four signals with equal amplitude and phase differences $\Delta\varphi_{12}$, $\Delta\varphi_{23}$ and $\Delta\varphi_{34}$ of 45°, 180°, and 135° between between ports 1 and 2, ports 2 and 3, and ports 3 and 4, respectively, the power will constructively recombine in port 1. If we increase $\Delta\varphi_{12}$, $\Delta\varphi_{23}$ and $\Delta\varphi_{34}$ with $-90°$, $-180°$, and $-270°$, respectively, the output signal will move to port 2. If the phase the phase differences are increased with the same amounts the signal moves to port 4, then to port 3, and then to port 1 again, and so on.

We will go through this sequence when the frequency is swept if the four branches of the MMI-PHASAR have length differences $\Delta L_{12}$, $\Delta L_{23}$, and $\Delta L_{34}$ which are related as $1:2:3$. These length differences can be obtained in different ways, as shown in Fig. 14.

The characteristics of MMI-PHASAR's differ from the classical PHASAR's in the following repsects:

- the response is inherently periodical;
- the channel response is very uniform (some nonuni-

formity is incurred by the transfer properties of the MMI-couplers);
- the low-crosstalk window is very narrow, which makes the component very sensitive to fabrication tolerances;
- flattening of the response is not possible.

For small numbers of wavelength channels MMI-PHASAR's can be very compact (e.g., 2800 $\mu$m $\times$ 100 $\mu$m for a four-channel demux [22]). The critical crosstalk preformance makes the device less attractive for applications as mux, demux or wavelength router. For application in a multiwavelength laser, where crosstalk performance is less relevant, the component has interesting properties. In this application, "chirping" of the array will be required in order to suppress undesired orders [26].

## VI. Conclusion

The application of PHASAR-based devices is rapidly broadening. PHASAR's have proven to be flexible components which support realization of a broad class of functions for use in multiwavelength networks. Silica-based devices offer the best performance and are presently being most widely applied. They might get some competition from polymer based devices in the future. InP-based devices are most promising for realization of active MW-devices such as MW-lasers and receivers and, on the longer term, for more complicated circuits containing large numbers of components, such as add-drops and optical crossconnects.

## Appendix A
## Waveguide Mode Effective Width

The diffraction properties of the phased array are conveniently expressed in terms of the effective mode width $w_e$ defined as the width of a uniform intensity distribution with the same maximum intensity and power content as the modal field

$$w_e = \frac{\int_{-\infty}^{+\infty} E(y)^2 dy}{E_{\max}^2}. \tag{A.1}$$

Substitution of the expression for the (TE-polarized) modal field [92] yields the following expression for $w_e$:

$$w_e = \frac{w_{\text{wg}}}{2} \cdot \left(1 + \frac{2}{v}\right) \approx w_{\text{wg}} \left(0.5 + \frac{1}{V - 0.6}\right) \tag{A.2}$$

in which $w_{\text{wg}}$ is the waveguide width and $V$ and $v$ are the normalized $V$-parameter and the normalized transverse attenuation constant, respectively. The rightmost expression, which is found empirically by curve fitting in the range $1 < V < 10$, gives us a simple expression for estimating the effective width.

Substitution of the Gaussian distribution $E(y) = E_0 \exp(-y^2/w_0^2)$ into (A.1) yields the following relation between $w_e$ and $w_0$.

$$w_0 = w_e \cdot \sqrt{2/\pi}. \tag{A.3}$$

Using (A.2) and (A.3), the modal field is easily "translated" into an equivalent Gaussian field.

## References


[1] R. Adar, C. H. Henry, C. Dragone, R. C. Kistler, and M. A. Milbrodt, "Broad-band array multiplexers made with silica waveguides on silicon," *J. Lightwave Technol.*., vol. 11, pp. 212–219, Feb. 1993.

[2] M. R. Amersfoort, M. K. Smit, Y. S. Oei, B. H. Verbeek, P. F. H. Groen, and E. G. Metaal, "Small-size, low-loss, 4-channel phased-array wavelength division (de)multiplexer on InP," in *Proc. 6th Eur. Conf. Integrated Optics (ECIO '93)*, Neuchatel, Switzerland, Apr. 18–22, 1993, pp. 2–5, postdeadline papers.

[3] M. R. Amersfoort, C. R. de Boer, Y. S. Oei, B. H. Verbeek, P. Demeester, F. H. Groen, and J. W. Pedersen, "High performance 4-channel PHASAR wavelength demultiplexer integrated with photodetectors," in *Proc. 19th Eur. Conf. Optical Communication (ECOC'93)*, Montreux, Switzerland, vol. 3, Sept. 12–16, 1993, pp. 49–52, postdeadline papers.

[4] M. R. Amersfoort, C. R. de Boer, B. H. Verbeek, P. Demeester, A. Looyen, and J. J. G. M. van der Tol, "Low-loss phased-array based 4-channel wavelength demultiplexer integrated with photodetectors," *IEEE Photon. Technol. Lett.*, vol. 6, pp. 62–64, Jan. 1994.

[5] M. R. Amersfoort, C. R. de Boer, F. P. G. M. van Ham, M. K. Smit, P. Demeester, J. J. G. M. van der Tol, and A. Kuntze, "Phased-array wavelength demultiplexer with flattened wavelength response," *Electron. Lett.*, vol. 30, no. 4, pp. 300–302, Feb. 1994.

[6] M. R. Amersfoort, J. B. D. Soole, H. P. Leblanc, N. C. Andreakakis, A. Rajhel, and C. Caneau, "8 × 2 nm polarization-independent WDM detector based on compact arrayed waveguide demultiplexer," *Integrated Photonics Research 1995*, Dana Point, CA, Feb. 23–25, 1995, pp. PD3-1–PD3-2, postdeadline papers.

[7] M. R. Amersfoort, J. B. D. Soole, H. P. Leblanc, N. C. Andreadakis, A. Rajhel, and C. Caneau, "Passband broadening of integrated arrayed waveguide filters using multimode interference couplers," *Electron. Lett.*, vol. 32, no. 5, pp. 449–451, Feb. 1996.

[8] M. R. Amersfoort, J. B. D. Soole, H. P. Leblanc, N. C. Andreakakis, A. Rahjel, C. Caneau, M. A. Koza, R. Bhat, C. Youtsey, and I. Adesida, "Polarization-independent InP-arrayed waveguide filter using square cross-section waveguides," *Optical Fiber Communication (OFC'96)*, Tech. Dig. Ser., San Jose, CA, Feb. 25–Mar. 1, 1996, pp. 101–102.

[9] M. R. Amersfoort, C. E. Zah, B. Pathak, F. Favire, P. S. D. Lin, A. Rahjel, N. C. Andreakakis, R. Bhat, C. Caneau, and M. A. Koza, "Wavelength accuracy and output power of multiwavelength DFB laser arrays with integrated star couplers and optical amplifiers," *Integrated Photonics Research 1996*, Boston, MA, Apr. 29–May 2, 1996, pp. 784–481.

[10] P. A. Besse, M. Bachmann, and H. Melchior, "Phase relations in multi-mode interference couplers and their application to generalized integrated Mach-Zehnder optical switches," in *Proc. 6th Eur. Conf. Integrated Optics (ECIO'93)*, Neuchatel, Switzerland, Apr. 18–22, 1993, pp. 2.22–2.23.

[11] H. Bissessur, F. Gaborit, B. Martin, P. Pagnod-Rossiaux, J.-L. Peyre, and M. Renaud, "16 Channel phased array demultiplexer on InP with low polarization sensitivity," *Electron. Lett.*, vol. 30, no. 4, pp. 336–337, Feb. 1994.

[12] H. Bissessur, F. Gaborit, B. Martin, G. Ripoche, and P. Pagnod-Rossiaux, "Tunable phased-array wavelength demultiplexer on InP," *Electron. Lett.*, vol. 31, no. 1, pp. 32–33, Jan. 1995.

[13] H. Bissessur, F. Gaborit, B. Martin, and G. Ripoche, "Polarization-independent phased-array demultiplexer on InP with high fabrication tolerance," *Electron. Lett.*, vol. 31, no. 16, pp. 1372–1373, Aug. 1995.

[14] H. Bissessur, B. Martin, R. Mestric, and F. Gaborit, "Small-size, polarization-independent phased-array demultiplexers on InP," *Electron. Lett.*, vol. 31, no. 24, pp. 2118–2120, Nov. 1995.

[15] H. Bissessur, P. Pagnod-Rossiaux, R. Mestric, and B. Martin, "Extremely small polarization independent phased-array demultiplexers on InP," *IEEE Photon. Technol. Lett.*, vol. 8, pp. 554–556, Apr. 1996.

[16] C. A. Brackett, "Dense wavelength division multiplexing networks: Principles and applications," *IEEE J. Select. Areas Commun.*, vol. 8, pp. 948–964, 1990.

[17] C. A. Brackett, A. S. Acampora, J. Sweitzer, G. Tangonan, M. T. Smith, W. Lennon, K. C. Wang, and R. H. Hobbs, "A scalable multiwavelength multihop optical network: A proposal for research on all-optical networks," *J. Lightwave Technol.*, vol. 11, pp. 736–753, May/June 1993.

[18] T. Brenner, C. H. Joyner, M. Zirngibl, and C. Doerr, "Compact waveguide grating array de-multiplexer," *Integrated Photonics Research 1996*, Boston, MA, pp. PDP3-1–PDP3-3, Apr. 29–May 2, 1996, postdeadline papers.

[19] K. S. Chiang, "Dispersion characteristics of strip dielectric waveguides," *IEEE Trans. Microwave Theory Tech.*, vol. 39, pp. 349–352, Feb. 1991.

[20] P. C. Clemens, G. Heise, R. Marz, H. Michel, A. Reichelt, and H. W. Schneider, "Optical phased array in $SiO_2$/Si with adaptable center wavelength," in *Proc. 7th Eur. Conf. Inegrated Optics (ECIO '95)*, Delft, The Netherlands, Apr. 3–6, 1995, pp. 505–508.

[21] P. C. Clemens, G. Heise, R. Marz, A. Reichelt, and H. W. Schneider, "Wavelength-adaptable optical phased array in $SiO_2$-Si," *IEEE Photon. Technol. Lett.*, vol. 7, pp. 1040–1041, Oct. 1995.

[22] C. van Dam, M. R. Amerfsoort, G. M. ten Kate, F. P. G. M. van Ham, M. K. Smit, P.A. Besse, M. Bachmann, and H. Melchior, "Novel InP-based phased-array wavelength demultiplexer using a generalized MMI-MZI configuration," in *Proc. 7th Eur. Conf. Integrated Optics (ECIO'95)*, Delft, The Netherlands, Apr. 3–6, 1995, pp. 275–278.

[23] C. van Dam, A. A. M. Staring, E. J. Jansen, J. J. M. Binsma, T. van Dongen, M. K. Smit, and B. H. Verbeek, "Loss reduction for phased-array demultiplexers using a double etch technique," *Integrated Photonics Research 1996*, Boston, MA, Apr. 29–May 2, 1996, pp. 52–55.

[24] S. Day, J. P. Stagg, D. Moule, S. J. Clemens, C. Rogers, S. Ohja, T. Clapp, J. Brook, and J. Morley, "The elimination of sidelobes in the arrayed waveguide WDM," *Integrated Photonics Research 1996*, Boston, MA, Apr. 29–May 2, 1996, pp. 48–51.

[25] C. R. Doerr, M. Zirngibl, and C. H. Joyner, "Chirping of the waveguide grating router for free-spectral-range mode selection in the multifrequency laser," *IEEE Photon. Technol. Lett.*, vol. 8, pp. 500–502, Apr. 1996.

[26] C. R. Doerr, M. Zirngibl, and C. H. Joyner, "Chirping of the waveguide grating router for free-spectral-range mode selection in the multifrequency laser," *Integrated Photonics Research 1996*, Boston, MA, pp. 132–135, Apr. 29–May 2, 1996.

[27] C. Dragone, "An $N \times N$ optical multiplexer using a planar arrangement of two star couplers," *IEEE Photon. Technol. Lett.*, vol. 3, pp. 812–815, Sept. 1991.

[28] C. Dragone, C. A. Edwards, and R. C. Kistler, "Integrated optics $N \times N$ multiplexer on silicon," *IEEE Photon. Technol. Lett.*, vol. 3, pp. 896–899, Oct. 1991.

[29] M. Fukui, K. Oda, H. Toba, K. Okamoto, and M. Ishii, "10 channel × 10Gbit/s WDM add/ drop multiplexing/transmission experiment over 240 km of dispersion-shifted fiber employing unequally-spaced arrayed-waveguide-grating ADM filter with fold-back configuration," *Electron. Lett.*, vol. 31, no. 20, pp. 1757–1759, Sept. 1995.

[30] B. Glance, I. P. Kaminow, and R. W. Wilson, "Applications of the integrated waveguide grating router," *J. Lightwave Technol.*, vol. 12, pp. 957–962, June 1994.

[31] B. R. Hemenway, M. L. Stevens, D. M. Castagozzi, D. Marquis, S. A. Parikh, J. J. Carney, S. G. Finn, E. A. Swanson, I. P Kaminow, C. Dragone, U. Koren, T. L. Koch, R. Thomas, C. Zveren, and E. Grella, "A 20-channel wavelength-routed all-optical network deployed in the Boston Metro area," *Optical Fiber Communication (OFC'95)*, Tech. Dig. Ser., San Diego, CA, Feb. 26–Mar. 3, 1995, pp. PD8-1–PD8-5, postdeadline papers.

[32] Y. Hida, Y. Innoue, and S. Imamura, "Polymeric arrayed-waveguide grating multiplexer operating around 1.3 $\mu$m," *Electron. Lett.*, vol. 30, no. 12, pp. 959–960, June 1994.

[33] Y. Innoue, Y. Ohmori, M. Kawachi, S. Ando, T. Sawada, and H. Takahashi, "Polarization mode converter with polyimide half waveplate in silica-based planar lightwave circuits," *IEEE Photon. Technol. Lett.*, vol. 6, pp. 626–628, May 1994.

[34] Y. Inoue, A. Himeno, K. Moriwaki, and M. Kawachi, "Silica-based arrayed-waveguide grating circuit as optical splitter/router," *Electron. Lett.*, vol. 31, no. 9, pp. 726–727, Apr. 1995.

[35] O. Ishida and H. Takahashi, "Loss-imbalance equalization of arrayed-waveguide grating add-drop multiplexer," *Electron. Lett.*, vol. 30, no. 14, pp. 1160–1162, July 1994.

[36] O. Ishida, H. Takahashi, and Y. Inoue, "FDM-channel selection filter employing an arrayed-waveguide grating multiplexer," *Electron. Lett.*, vol. 30, no. 16, pp. 1327–1328, Aug. 1994.

[37] O. Ishida, H. Takahashi, S. Suzuki, and Y. Innoue, "Multichannel frequency-selective switch employing an arrayed-waveguide grating multiplexer with fold-back optical paths," *IEEE Photon. Technol. Lett.*, vol. 6, pp. 1219–1221, Oct. 1994.

[38] O. Ishida, T. Hasegawa, M. Ishii, S. Suzuki, and K. Iwashita, "4 × 4, 7-FDM-channel reconfigurable network hub emplying arrayed-waveguide-grating (AWG) multiplexers," *Optical Fiber Communication (OFC'95)*, Tech. Dig. Ser., San Diego, USA, Feb. 26–Mar. 3, 1995, pp. PD9-1–PD9-5, postdeadline papers.

[39] C. H. Joyner, M. Zirngibl, and J. P. Meester, "A multifrequency waveguide grating laser by selective area epitaxy," *IEEE Photon. Technol. Lett.*, vol. 6, pp. 1277–1279, Nov. 1994.

[40] C. H. Joyner, M. Zirngibl, and J. C. Centanni, "An 8 channel digitally tunable transmitter with electroabsorption modulated output by selective area epitaxy," *Integrated Photonics Research 1995*, Dana Point, CA, Feb. 23–25, 1995, pp. PD2-2–PD2-4, postdeadline papers.

[41] ——, "An 8-channel digitally tunable transmitter with electroabsorption modulated output by selective-area epitaxy," *IEEE Photon. Technol. Lett.*, vol. 7, pp. 1013–1015, Sept. 1995.

[42] L. O. Lierstuen and A. Sudbo, "8-channel wavelength division multiplexer based on multimode interference couplers," *IEEE Photon. Technol. Lett.*, vol. 7, pp. 1034–1036, Sept. 1995.

[43] R. März, *Integrated Optics: Design and Modeling*. Norwood, MA: Artech House, 1994.

[44] R. Mestric, H. Bissessur, B. Martin, and A. Pinquier, "1.31–1.55-$\mu$m phased-array demultiplexer on InP," *IEEE Photon. Technol. Lett.*, vol. 8, pp. 638–640, May 1996.

[45] aR. Mestric, M. Renaud, B. G. Martin, and F. Gaborit, "Extremely compact 1.31–1.55 $\mu$m phased array duplexer on InP with $-30$ dB crosstalk over 100 nm," in *Proc. 22nd Eur. Conf. Optical Communication (ECOC'96)*, Oslo, Sweden, Sept. 15–19, 1996, pp. 3.131–3.134.

[46] K. Okamoto and H. Yamada, "Arrayed-waveguide grating multiplexer with flat spectral response," *Opt. Lett.*, vol. 20, no. 1, pp. 43–45, Jan. 1995.

[47] K. Okamoto, K. Moriwaki, and S. Suzuki, "Fabrication of $64 \times 64$ arrayed-waveguide grating multiplexer on silicon," *Electron. Lett.*, vol. 31, no. 3, pp. 184–186, Feb. 1995.

[48] K. Okamoto, K. Takiguchi, and Y. Ohmori, "16ch optical add/drop multiplexer using silica-based arrayed-waveguide gratings," *Optical Fiber Communication (OFC'95)*, Tech. Dig. Ser., San Diego, CA, Feb. 26–Mar. 3, 1995, pp. PD10-1–PD10-5, postdeadline papers.

[49] K. Okamoto, K. Takiguchi, and Y. Ohmori, "16-channel add/drop multiplexer using silica-based arrayed-waveguide gratings," *Electron. Lett.*, vol. 31, no. 9, pp. 723–724, Apr. 1995.

[50] K. Okamoto, M. Ishii, Y. Hibino, and H. Toba, "Fabrication of unequal channel spacing arrayed-waveguide grating multiplexer modules," *Electron. Lett.*, vol. 31, no. 17, pp. 1464–1465, Aug. 1995.

[51] K. Okamoto, M. Ishii, Y. Hibino, and Y. Ohmori, "Fabrication of variable bandwidth filters using arrayed-waveguide gratings," *Electron. Lett.*, vol. 31, no. 18, pp. 1592–1594, Aug. 1995.

[52] K. Okamoto, M. Okuno, A. Himeno, and Y. Ohmori, "16-channel optical add/drop multiplexer consisting of arrayed-waveguide gratings and double-gate switches," *Electron. Lett.*, vol. 32, no. 16, pp. 1471–1472, Aug. 1996.

[53] H. Okayama and M. Kawahara, "Waveguide array grating demultiplexer on $LiNbO_3$," *Integrated Photonics Research 1995*, Dana Point, CA, pp. 296–298, Feb. 23–25, 1995.

[54] H. Okayama, M. Kawahara, and T. Kamijoh, "Reflective waveguide array demultiplexer in $LiNbO_3$," *J. Lightwave Technol.*, vol. 14, pp. 985–990, June 1996.

[55] E. C. M. Pennings, J. Van Schoonhoven, J. W. M. Van Uffelen, and M. K. Smit, "Reduced bend-ing and scattering losses in new optical 'double-ridge' waveguide," *Electron. Lett.*, vol. 25, no. 11, pp. 746–747, May 1989.

[56] E. C. M. Pennings, M. K. Smit, and G. D. Khoe, "Micro-Optic versus waveguide devices—An Overview," invited paper, in *Proc. Fifth MicroOptics Conf. 1995*, Hiroshima, Japan, Oct. 18–20, 1995, pp. 248–255.

[57] E. C. M. Pennings, M. K. Smit, A. A. M. Staring, and G.-D. Khoe, "Integrated-Optics versus Micro-Optics—A comparison," *Integrated Photonics Research IPR'96*, Boston, MA, Tech. Dig., vol. 6, Apr. 29–May 2, 1996, pp. 460–463.

[58] M. K. Smit, "Now focussing and dispersive planar component based on an optical phased array," *Electron. Lett.*, vol. 24, no. 7, pp. 385–386, Mar. 1988.

[59] ——, "Optical phased arrays," in Integrated Optics in Silicon-Based Aluminum Oxide, Ph.D. thesis, Delft Univ. of Technol., 1991, ch 6.

[60] L. B. Soldano, M. Bouda, M. K. Smit, and B. H. Verbeek, "New small-size single-mode optical power splitter based on multi-mode interference," in *Proc. 18th Eur. Conf. Optical Communiction (ECOC '92)*, Berlin, Germany, Sept. 27–Oct. 1, 1992, pp. 465–468.

[61] L. B. Soldano and E. C. M. Pennings, "Optical multi-mode interference devices based on self-imaging: principles and applications," *J. Lightwave Technol.*, vol. 13, pp. 615–627, Apr. 1995.

[62] J. B. D. Soole, M. R. Amersfoort, H. P. Leblanc, N. C. Andreadakis, A. Rajhel, and C. Caneau, "Polarization-independent monolithic eight-channel 2 nm spacing WDM receiver detector based on compact arrayed waveguide demultiplexer," *Electron. Lett.*, vol. 31, no. 15, pp. 1289–1291, July 1995.

[63] J. B. D. Soole, M. R. Amersfoort, H. P. Leblanc, N. C. Andreadakis, A.

Rajhel, C. Caneau, M. A. Koza, R. Bhat, C. Youtsey, and I. Adesida, "Polarization-independent InP arrayed waveguide filter using square cross-section waveguides," *Electron. Lett.*, vol. 32, no. 4, pp. 323–324, Feb. 1996.

[64] J. B. D. Soole, M. R. Amersfoort, H. P. Leblanc, N. C. Andreakakis, A. Rajhel, C. Caneau, R. Bhat, and M. A. Koza, "Use of multimode interference couplers to broaden the passband of dispersive integrated WDM filters," *Integrated Photonics Research 1996*, Boston, MA, Apr. 29–May 2, 1996, pp. 44–47.

[65] J. B. D. Soole, M. R. Amersfoort, H. P. Leblanc, N. C. Andreadakis, A. Rajhel, C. Caneau, R. Bhat, M. A. Koza, C. Youtsey, and I. Adesida, "Use of multimode interference couplers to broaden the passband of wavelength-dispersive integrated WDM filters," *IEEE Photon. Technol. Lett.*, vol. 8, pp. 1340–1342, Oct. 1996.

[66] L. H. Spiekman, F. P. G. M. van Ham, A. Kuntze, J.W. Pedersen, P. Demeester, and M. K. Smit, "Polarization-independent InP-based phased-array wavelength demultiplexer with flattened wavelength response," in *Proc. 20th Eur. Conf. Optical Communication (ECOC'94)*, Firenze, Italy, Sept. 25–29, 1994, pp. 759–762.

[67] L. H. Spiekman, A. H. de Vreede, F. P. G. M. van Ham, A. Kuntze, J. J. G. M. Van der Tol, P. Demeester, and M. K. Smit, "Flattened response ensures polarization independence of InGaAsP/InP phased array wavelength demultiplexer," in *Proc. 7th Eur. Conf. Integrated Optics (ECIO'95)*, Delft, The Netherlands, Apr. 3–6, 1995, pp. 517–520.

[68] L. H. Spiekman, A. A. M. Staring, C. van Dam, E. J. Jansen, J. J. M. Binsma, M. K. Smit, and B. H. Verbeek, "Space-switching using wavelength conversion at 2.5 Gb/s and integrated phased array routing," in *Proc. Eur. Conf. Optical Communications (ECOC'95)*, Brussels, Belgium, Sept. 17–21, 1995, pp. 1055–1058, postdeadline papers.

[69] L. H. Spiekman, M. B. J. Diemeer, T. H. Hoekstra, and M. K. Smit, "First polymeric phased array wavelength demultiplexer operating at 1550 nm," *Integrated Photonics Research 1996*, Boston, MA, Apr. 29–May 2, 1996, pp. 36–39.

[70] L. H. Spiekman, A. A. M. Staring, J. J. M. Binsma, E. J. Jansen, T. van Dongen, P. J. A. Thijs, M. K. Smit, and B. H. Verbeek, "A compact phased array based multi-wavelength laser," *Integrated Photonics Research 1996*, Boston, MA, Apr. 29–May 2, 1996, pp. 136–138.

[71] L. H. Spiekman, M. R. Amersfoort, A. H. de Vreede, F. P. G. M. van Ham, A. Kuntze, J. W. Pedersen, P. Demeester, and M. K. Smit, "Design and realization of polarization independent phased array wavelength demultiplexers using different array orders for TE and TM," *J. Lightwave Technol.*, vol. 14, pp. 991–995, June 1996.

[72] A. A. M. Staring, L. H. Spiekman, C. van Dam, E. J. Jansen, J. J. M. Binsma, M. K. Smit, and B. H. Verbeek, "Space-switching 2.5 Gbit/s signals using wavelength conversion and phased array routing," *Electron. Lett.*, vol. 32, no. 4, pp. 377–379, Feb. 1996.

[73] A. A. M. Staring, L. H. Spiekman, J. J. M. Binsma, E. J. Jansen, T. van Dongen, P. J. A. Thijs, M. K. Smit, and B. H. Verbeek, "A compact 9 channel multi-wavelength laser," *IEEE Photon. Technol. Lett.*, vol. 8, pp. 1139–1141, Sept. 1996.

[74] C. A. M. Steenbergen, C. van Dam, T. L. M. Scholtes, A. H. de Vreede, L. Shi, J. J. G. M. van der Tol, P. Demeester, and M. K. Smit, "4-channel wavelength flattened demultiplexer integrated with photodetectors," in *Proc. 7th Eur. Conf. Integrated Optics (ECIO '95)*, Delft, The Netherlands, Apr. 3–6, 1995, pp. 271–274.

[75] C. A. M. Steenbergen, C. van Dam, A. H. de Vreede, L. Shi, J. W. Pedersen, P. Demeester, and M. K. Smit, "Integrated 1 GHz 4-channel InP phasar based WDM-receiver with Si bi-polar frontend array," in *Proc. Eur. Conf. Optical Communications (ECOC'95)*, Brussels, Belgium, Sept. 17–21, 1995, pp. 211–214.

[76] C. A. M. Steenbergen, M. O. van Deventer, L. C. N. de Vreede, C. van Dam, M. K. Smit, and B. H. Verbeek, "System performance of a 4 channel phasar WDM receiver operating at 1.2 Gb/s," *Optical Fiber Communication (OFC'96)*, Tech. Dig. Ser., San Jose, CA, Feb. 25–Mar. 1, 1996, pp. 310–311.

[77] C. A. M. Steenbergen, C. van Dam, A. Looijen, C. G. P. Herben, M. de Kok, M. K. Smit, J. W. Pedersen, I. Moerman, R. G. Baets, and B. H. Verbeek, "Compact low loss 8 $\times$ 10 GHz polarization independent WDM receiver," in *Proc. 22nd Eur. Conf. Optical Communication (ECOC'96)*, Oslo, Sweden, Sept. 15–19, 1996, pp. 1.129–1.132.

[78] S. Suzuki, Y. Innoue, and Y. Ohmori, "Polarization-insensitive arrayed-waveguide grating multiplexer with $SiO_2$-on-$SiO_2$ structure," *El. Lett.*, vol. 30, no. 8, pp. 642–643, Apr. 1994.

[79] S. Suzuki, A. Himeno, Y. Tachikawa, and Y. Yamada, "Multichannel optical wavelength selective switch with arrayed-waveguide grating multiplexer," *Electron. Lett.*, vol. 30, no. 13, pp. 1091–1092, June 1994.

[80] Y. Tachikawa, Y. Inoue, M. Kawachi, H. Takahashi, and K. Inoue, "Arrayed-waveguide grating add-drop multiplexer with loop-back optical paths," *Electron. Lett.*, vol. 29, no. 24, pp. 2133–2134, Nov. 1993.

[81] Y. Tachikawa and M. Kawachi, "Lightwave transrouter based on arryed-waveguide grating multiplexer," *Electron. Lett.*, vol. 30, no. 18, pp. 1504–1506, Sept. 1994.

[82] Y. Tachikawa, M. Ishii, Y. Inoue, and T. Nozawa, "Integrated-optic arrayed-waveguide grating multiplexers with loop-back optical paths," in *Proc. 7th Eur. Conf. Int. Opt. (ECIO '95)*, Delft, The Netherlands, Apr. 3–6, 1995, pp. 267–270.

[83] Y. Tachikawa and K. Okamoto, "32 wavelength tunable arrayed-waveguide grating laser based on special input/output arrangement," *Electron. Lett.*, vol. 31, no. 19, pp. 1665–1666, Sept. 1995.

[84] Y. Tachikawa and Y. Inoue, "Tunable WDM-channel group drop filters based on smart device configuration," *Electron. Lett.*, vol. 31, no. 23, pp. 2029–2030, Nov. 1995.

[85] Y. Tachikawa, Y. Inoue, M. Ishii, and T. Nozawa, "Arreyed-waveguide grating multiplexer with loop-back optical paths and its applications," *J. Lightwave Technol.*, vol. 14, pp. 977–984, June 1996.

[86] K. Takada, Y. Inoue, H. Yamada, and M. Horiguchi, "Measurement of phase error distributions in silica-based arrayed-waveguide grating multiplexers by using Fourier transform spectroscopy," *Electron. Lett.*, vol. 30, no. 20, pp. 1671–1672, Sept. 1994.

[87] H. Takahashi, S. Suzuki, K. Kato, and I. Nishi, "Arrayed-waveguide grating for wavelength division multi/demultiplexer with nanometer resolution," *Electron. Lett.*, vol. 26, no. 2, pp. 87–88, Jan. 1990.

[88] H. Takahashi, I. Nishi, and Y. Hibino, "10 GHz spacing optical frequency division multiplexer based on arrayed-waveguide grating," *Electron. Lett.*, vol. 28, no. 4, pp. 380–382, Feb. 1992.

[89] H. Takahashi, Y. Hibino, and I. Nishi, "Polarization-insensitive arrayed-waveguide grating wavelength multiplexer on silicon," *Opt. Lett.*, vol. 17, no. 7, pp. 499–501, Apr. 1992.

[90] H. Takahashi, Y. Hibino, Y. Ohmori, and M. Kawachi, "Polarization-insensitive arrayed-waveguide wavelength demultiplexer with birefringence compensating film," *IEEE Photon. Technol. Lett.*, vol. 5, pp. 707–709, June 1993.

[91] H. Takahashi, K. Oda, H. Toba, and Y. Inoue, "Transmission characteristics of arrayed waveguide $N \times N$ wavelength multiplexer," *J. Lightwave Technol.*, vol. 13, pp. 447–455, Mar. 1995.

[92] H. G. Unger, *Planar Optical Waveguides and Fibers*. Oxford, U.K.: Clarendon Press, Oxford Engineering Science Series, 1977.

[93] A. R. Vellekoop and M. K. Smit, "Low-loss planar optical polarization splitter with small dimensions," *Electron. Lett.*, vol. 25, pp. 946–947, 1989.

[94] ——, "A polarization independent planar wavelength demulti- plexer with small dimensions," in *Proc. Eur. Conf. Opt. Integrated Systems*, Amsterdam, The Netherlands, Sept. 25–28, 1989, paper D3.

[95] A. R. Vellekoop and M. K. Smit, "Four-channel integrated-optic wavelength demultiplexer with weak polarization dependence," *J. Lightwave Technol.*, vol. 9, no. 3, pp. 310–314, Mar. 1991.

[96] B. H. Verbeek, A. A. M. Staring, E. J. Jansen, R. van Roijen, J. J. M. Binsma, T. van Dongen, M. R. Amersfoort, C. van Dam en, and M. K. Smit, "Large bandwidth polarization independent and compact 8 channel PHASAR demultiplexer/filter," *Optical Fiber Communication (OFC'94)*, Tech. Dig. Ser., San Jose, CA, Feb. 20–25, 1994, pp. 63–66, postdeadline papers.

[97] B. Verbeek and M. K. Smit, "Phased array based WDM devices," in *Proc. Eur. Conf. on Optical Communication (ECOC'95)*, Brussels, Belgium, Sept. 17–21, 1995, pp. 195–202.

[98] C. G. M. Vreeburg, C. R. de Boer, Y. S. Oei, B. H. Verbeek, R. T. H. Rongen, H. Vonk, M. R. Leys, and J. H. Wolter, "Strained InP/InGaAs quantum well layers for wavelength demultiplexers," in *Procs. 7th Eur. Conf. Integrated Optics (ECIO'95)*, Delft, The Netherlands, Apr. 3–6, 1995, pp. 283–286.

[99] C. G. M. Vreeburg, T. Uitterdijk, Y. S. Oei, M. K. Smit, F. H. Groen, J. J. G. M. van der Tol, P. Demeester, and H. J. Frankena, "Compact integrated InP-based add-drop multiplexer," in *Proc. 22nd Eur. Conf. Optical Communication (ECOC'96)*, Oslo, Sweden, Sept. 15–19, 1996, pp. 5.67–5.70.

[100] I. H. White, K. O. Nyairo, P. A. Kirkby, and C. J. Armistead, "Demonstration of a 1 $\times$ 2 multichannel grating cavity laser for wavelength division multiplexing (WDM) applications," *Electron. Lett.*, vol. 26, no. 13, pp. 832–834, June 1990.

[101] H. Yamada, K. Takada, Y. Inoue, Y. Hibino, and M. Hroiguchi, "10 GHz-spaced arrayed-waveguide grating multiplexer with phase-error-compensating thin-film heaters," *Electron. Lett.*, vol. 31, no. 5, pp. 360–361, Mar. 1995.

[102] H. Yamada, K. Takada, Y. Inoue, Y. Ohmori, and S. Mitachi, "Statically-phase-compensated 10 GHz spaced arrayed-waveguide grating," *Electron. Lett.*, vol. 32, no. 17, pp. 1580–1582, Aug. 1996.

[103] M. G. Young, U. Koren, B. I. Miller, M. Chien, T. L. Koch, D. M. Tennant, K. Feder, K. Dreyer, and G. Raybon, "Six wavelength laser array with integrated amplifier and modulator," *Electron. Lett.*, vol. 31, no. 21, pp. 1835–1836, Oct. 1995.

[104] C. E. Zah, F. J. Favire, B. Pathak, R. Bhat, C. Caneau, P. S. D. Lin, A. S. Gozdz, N. C. Andreakakis, M. A. Koza, and T. P. Lee, "Monolithic integration of multiwavelength compressive-strained multiquantum-well distributed-feedback laser array with star coupler and optical amplifiers," *Electron. Lett.*, vol. 28, no. 25, pp. 2361–2362, Dec. 1992.

[105] F. Zamkotsian, H. Okamoto, K. Kishi, M. Okamoto, Y. Yoshikuni, K. Sato, and K. Oe, "An InP-based optical multiplexer for 100-GHz pulse-train generation," *IEEE Photon. Technol. Lett.*, vol. 7, pp. 502–504, May 1995.

[106] M. Zirngibl, C. Dragone, and C. H. Joyner, "Demonstration of a 15 $\times$ 15 arrayed waveguide multiplexer on InP," *IEEE Photon. Technol. Lett.*, vol. 4, pp. 1250–1253, Nov. 1992.

[107] M. Zirngibl, C. H. Joyner, L. W. Stulz Th. Gaiffe, and C. Dragone, "Polarization independent 8 $\times$ 8 waveguide grating multiplexer on InP," *Electron. Lett.*, vol. 29, no. 2, pp. 201–202, Jan. 1993.

[108] M. Zirngibl and C. H. Joyner, "12 frequency WDM laser based on a transmissive waveguide grating router," *Electron. Lett.*, vol. 30, no. 9, pp. 701–702, Apr. 1994.

[109] M. Zirngibl, C. H. Joyner, and B. Glance, "Digitally tunable channel dropping filter/ equalizer based on waveguide grating router and optical amplifier integration," *IEEE Photon. Technol. Lett.*, vol. 6, pp. 513–515, Apr. 1994.

[110] M. Zirngibl, C. H. Joyner, L. W. Stulz, U. Koren, M.-D. Chien, M. G. Young, and B. I. Miller, "Digitally tunable laser based on a waveguide grating multiplexer and an optical amplifier," *IEEE Photon. Technol. Lett.*, vol. 6, pp. 516–518, Apr. 1994.

[111] M. Zirngibl, C. H. Joyner, and L. W. Stulz, "Demonstration of 9 $\times$ 200 Mbit/s wavelength division multiplexed transmitter," *Electron. Lett.*, vol. 30, no. 18, pp. 1484–1485, Sept. 1994.

[112] M. Zirngibl, B. Glance, L. W. Stulz, C. H. Joyner, G. Raybon, and I. P. Kaminow, "Characterization of a multiwavelength waveguide grating router laser," *IEEE Photon. Technol. Lett.*, vol. 6, pp. 1082–1084, Sept. 1994.

[113] M. Zirngibl, C. H. Joyner, and L. W. Stulz, "WDM receiver by monolithic integration of an optical preamplifier, waveguide grating router and photodiode array," *Electron. Lett.*, vol. 31, no. 7, pp. 581–582, Mar. 1995.

[114] M. Zirngibl, C. H. Joyner, and P. C. Chou, "Polarization compensated waveguide grating router on InP," *Electron. Lett.*, vol. 31, no. 19, pp. 1662–1664, Sept. 1995.

[115] M. Zirngibl, C. H. Joyner, C. R. Doerr, L. W. Stulz, and H. M. Presby, "A 18 channel multi frequency laser," *Integrated Photonics Research 1996*, Boston, MA, Apr. 29–May 2, 1996, pp. 128–131.

**Meint K. Smit**, for photograph and biography, see this issue, p. 150.

**Cor van Dam** was born in the Hague, The Netherlands, in 1967. He received the master's degree in electrical engineering from the Delft University of Technology, in 1990.

His thesis research was carried out in the Integrated Optics group of the Laboratory of Telecommunication and Remote Sensing Technology and concerned the development of an CAD-tool for the design and analysis of photonic integrated circuits, using a microwave design system. In 1991, he was appointed to the scientific staff of the laboratory where he is currently carrying out his Ph.D. research which involves development of polarization independent integrated wavelength division demultiplexers.